

Tetragonal to Orthorhombic Transition of GdFeAsO Studied by Single-Crystal Synchrotron X-Ray Diffraction

F. Nitsche,¹ Th. Doert,^{1,*} and M. Ruck^{1,2}

¹Department of Chemistry and Food Chemistry, Technische Universität Dresden, D-01062 Dresden, Germany

²Max Planck Institute for Chemical Physics of Solids, D-01187 Dresden, Germany

(Dated: February 21, 2022)

A study of the tetragonal to orthorhombic phase transition of GdFeAsO is presented. Planes of the reciprocal space were reconstructed from single-crystal synchrotron X-ray diffraction data. By cooling below the structural transition temperature splitting of the Bragg reflections was observed corresponding to four different twin domain orientations. A model was developed to quantify the distortion of the lattice from the position of the splitted reflections relative to each other. Constrained 2D-Cauchy fits of several splitted reflections provided positions of the reflections. The influence of the structural distortion was detectable already above the structural transition temperature hinting at fluctuations in the tetragonal phase.

PACS numbers: 61.50.Ks 61.66.Fn, 74.62.Bf, 74.70.Xa,

Keywords: Fe-based superconductors, synchrotron x-ray diffraction, phase transition, twinning, single crystal

I. INTRODUCTION

With the discovery of high-temperature superconductivity in layered iron containing compounds (iron pnictides)^{1–3}, a new system of phases was added to the study of unconventional superconductivity. Since the understanding of the phenomenon of high- T_c superconductivity is still limited, the question of the differences and similarities towards other high- T_c compounds such as the cuprates arises⁴.

The cuprates as well as many iron pnictides become superconducting by doping of a non-superconducting antiferromagnetic “parent” compound. Whereas the superconductivity in the cuprates is believed to originate from the Mott-insulator properties of the “parent” compound, the iron pnictides do not exhibit this electronic correlation. However, a common feature is the antiferromagnetic ordering, which has to be suppressed to achieve superconductivity and is thus considered significant.

Iron pnictides, such as $REFeAsO$, (RE = rare-earth metal) and AFe_2As_2 (A = Ca, Sr, Ba, and Eu), show antiferromagnetic transitions accompanied by structural distortions from tetragonal to orthorhombic symmetry upon cooling. While the structural transition and the magnetic ordering occur simultaneously in AFe_2As_2 ^{5,6}, the structural transition in $REFeAsO$ compounds is observed at slightly higher temperatures than the magnetic ordering^{7–11}.

The $REFeAsO$ room-temperature phases of $ZrCuSiAs$ -type structure (space-group type $P4/nmm$) undergo a *translationengleiche* transition of index 2 to the low-temperature structure with space-group type $Cmme$ ⁷ (Fig. 1, for structural relations see also Ref. 12). A similar transition occurs in the AFe_2As_2 compounds ($I4/mmm$ to $Fmmm$). Tanatar *et al.*¹³ and Blomberg *et al.*¹⁴ studied the formation of lamellar transformation twins by single-crystal X-ray diffraction of AFe_2As_2 and the influence of the domain structure on the anisotropy

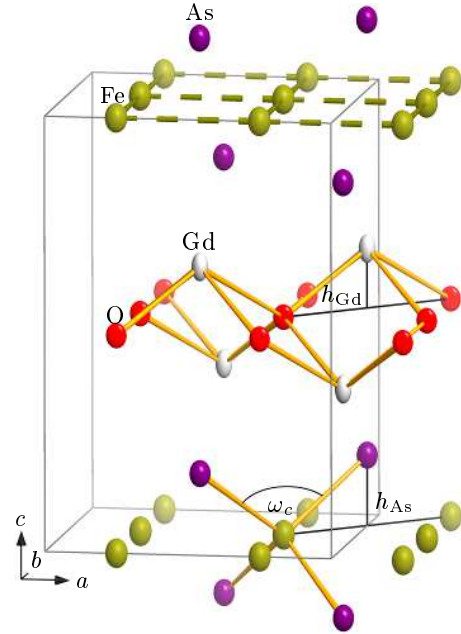


FIG. 1. (Color online) Low-temperature crystal structure of GdFeAsO at 50 K (space group $Cmme$, No. 67). The displacement ellipsoids represent 99.9% probability. Solid lines between iron atoms indicate shortest Fe-Fe distance, dashed lines are slightly longer. h_{Gd} is the height of gadolinium ions above the oxygen layer, h_{As} is the height of the arsenic ions above the iron layer, and ω_c is the As-Fe-As angle with the angle bisector parallel to the c -direction.

of the resistivity in directions of the basal plane. Due to the analogous mechanism of the structural transition for $REFeAsO$, the question arises, if the twin formation is similar to AFe_2As_2 .

Here, we present the first single-crystal X-ray diffraction study of the structural evolution and the twin formation of $REFeAsO$ compounds with GdFeAsO as rep-

representative. Doped GdFeAsO has one of the highest T_c (56 K) in this class of superconductors¹⁵, which has been associated with the vanishing distortion of the FeAs₄ tetrahedra¹⁶. This concept has been the starting point of an ongoing investigation on the structural changes associated with the transition to the superconducting phase and its physical implications.

II. EXPERIMENTAL

Preparation and characterization of the crystal used for single-crystal synchrotron X-ray diffraction has been described elsewhere¹⁷. Diffraction data for this study were recorded with a 165 mm MAR-CCD detector mounted on a Huber four-circle diffractometer at beamline D3 at DESY. The measurements were performed in the temperature range of 50–300 K using an open flow Oxford Diffraction Helijet cryostat. φ -scans were recorded with an increment of 1° , a detector distance of 54.4 mm, and a wavelength of 0.49741 Å. The detector distance and the wavelength were refined by comparing the experimental lattice parameters of a standard corundum single-crystal to literature data. The raw frames from the MAR-CCD detector were converted using the APEXII suite¹⁸. Integration and corrections for oblique incidence and polarization were performed within SAINT+¹⁹. For data reduction and absorption correction SADABS²⁰ was used. The structures were solved and refined with SHELXS and SHELXL²¹. Details concerning the structure analysis of GdFeAsO at different temperatures can be obtained from the Fachinformationszentrum Karlsruhe²².

III. RESULTS AND DISCUSSION

When cooling below the temperature of the structural transition, $T_s \approx 115$ K, splitting of reflections at high diffraction angles was observed in the synchrotron experiment. To assess the metric distortion during the structural transition, a program was written in MATLAB²³, that allows reconstruction of planes of the reciprocal space with high lateral resolution (Fig. 2).

The metric distortion of the structure is the only degree of freedom generated by the structural transition. A model has been developed, which allows to determine the metrical distortion from the observed splitting of reflections. For convenient comparison of the tetragonal (indicated by subscript t) and orthorhombic (subscript o) structures, the C -centered orthorhombic cell is transformed into a monoclinic (subscript m) primitive cell (upper right panel in Fig. 3) by

$$\mathbf{a}_m = \frac{1}{2}(\mathbf{a}_o + \mathbf{b}_o) \text{ and } \mathbf{b}_m = \frac{1}{2}(-\mathbf{a}_o + \mathbf{b}_o) \\ \text{with } |\mathbf{a}_m| = |\mathbf{b}_m| \text{ and } |\mathbf{a}_o| > |\mathbf{b}_o|.$$

The distortion of the structure is then defined by the angle $\gamma > 90^\circ$ (i.e. $\gamma^* < 90^\circ$ in reciprocal space).

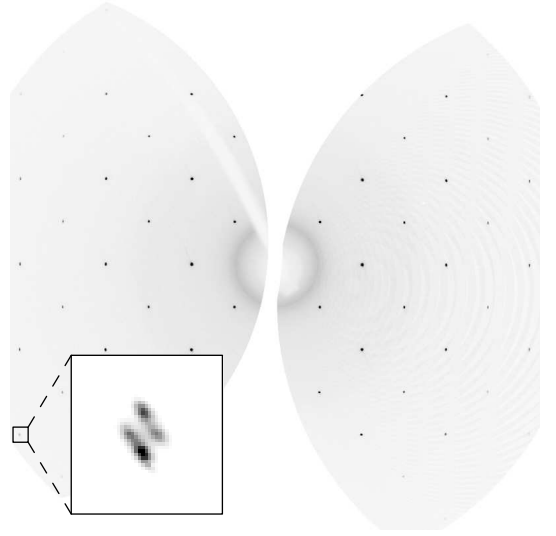


FIG. 2. Reconstructed $h k 0$ plane in monoclinic indexing of GdFeAsO at 50 K. *Inset*: Magnification of the $\bar{6} 4 0$ reflections.

The twin domains join in common planes that are indexed (110) and $(1\bar{1}0)$ in the C -centered cell, i.e. (100) and (010) in the primitive cell. Thus four different orientations of the domains in the low-temperature phase result. In the diffraction pattern fourfold splitting of reflections in general positions can be observed, especially at higher diffraction angles (Inset in Fig. 2). The position vectors \mathbf{p}_1 , \mathbf{p}_2 , \mathbf{p}_3 , and \mathbf{p}_4 of the reflections belonging to the four domains can be derived from their common center \mathbf{p}_c and the distortion angle γ^* (Fig. 3) by

$$\mathbf{p}_1 = \begin{pmatrix} 1 & -\sin(\gamma^* - 90^\circ) \\ 0 & \cos(\gamma^* - 90^\circ) \end{pmatrix} \mathbf{p}_c, \mathbf{p}_2 = \begin{pmatrix} 1 & \sin(\gamma^* - 90^\circ) \\ 0 & \cos(\gamma^* - 90^\circ) \end{pmatrix} \mathbf{p}_c, \\ \mathbf{p}_3 = \begin{pmatrix} \cos(\gamma^* - 90^\circ) & 0 \\ -\sin(\gamma^* - 90^\circ) & 1 \end{pmatrix} \mathbf{p}_c, \mathbf{p}_4 = \begin{pmatrix} \cos(\gamma^* - 90^\circ) & 0 \\ \sin(\gamma^* - 90^\circ) & 1 \end{pmatrix} \mathbf{p}_c.$$

Blomberg *et al.*¹⁴ detwinned BaFe₂As₂ crystals by tensile stress and showed that the relative positions of the reflections is dependent on the domain fractions. If, for example, the domain fraction of D4 in Fig. 3 increases, the orientation of the two sets of domains changes towards each other. In the geometrical model described here, the correlation of the reflection positions to their intensity is achieved by linear scaling of the transformations shown above. This approximation is acceptable due to the small differences of the intensities and the local fit of the reflections. In summary, the positions of the reflections are constrained to their common center \mathbf{p}_c of all the four reflections, the monoclinic distortion angle γ^* , and the intensities of the reflections. This enables the parameter refinement of overlapping reflections.

To quantify the distortion, an algorithm was written in MATLAB to fit the splitted reflections by a linear combination of four elliptical 2D-Lorentz (Cauchy) functions (concerning multivariate t-distributions see Ref. 24, 2D-Gaussian fit of neutron data see Refs. 25 and 26). A

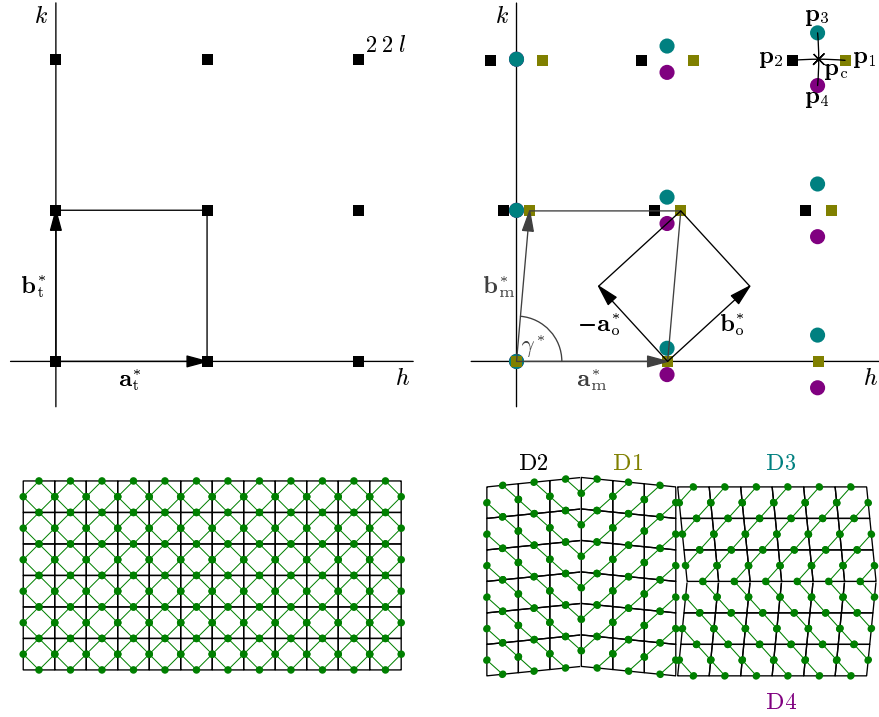


FIG. 3. (Color online) Scheme of the tetragonal (left) to orthorhombic (right) distortion in analogy to Ref. 13. *Upper panels:* Schematic reflection patterns for a^*b^* -planes with $l \neq 0$. *Lower panels:* Real space domains. Black lines represent the primitive unit cells, green points are the positions of iron atoms and green lines show shortest Fe-Fe distance. D1 to D4 denote the domain orientations corresponding to p1 to p4 in the upper right panel.

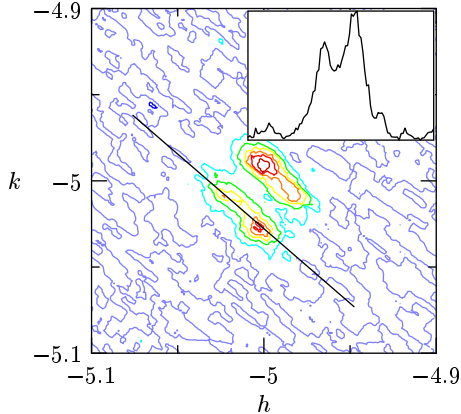


FIG. 4. (Color online) Contour plot of the $\bar{5}\bar{5}0$ reflection in $hk0$ plane. *Inset:* 1D-section of the 2D-distribution as indicated by the black line in the contour plot.

Lorentzian type profile function was chosen empirically by investigating 1D-sections of the 2D-distribution (see Fig. 4). The fitting parameters were the center of the splitted reflections \mathbf{p}_c , the distortion angle (γ^*), the ellipticity of the reflections, the width of the 2D-Lorentz distributions, and the individual intensities of the reflections.

For the structural investigation 20 reflections of each measurement, exhibiting reflection splitting, were fitted

to obtain an average distortion angle γ^* and a corresponding standard deviation. The reflection data were integrated with a tetragonal cell since splitting was not wide enough to perform multidomain integration. Using the tetragonal lattice parameters, which correspond to \mathbf{p}_c , and the obtained distortion angle, the orthorhombic lattice parameters were obtained by

$$a_o = 2 a_t \sin\left(\frac{\gamma}{2}\right) \text{ and } b_o = 2 a_t \cos\left(\frac{\gamma}{2}\right).$$

All reflections could be fitted with this model. No signs for a deviation from the low-temperature orthorhombic structure towards true monoclinic symmetry was observed. Furthermore, no superstructure reflections could be identified in the reconstructed images of the reciprocal space. This confirms the tetragonal to orthorhombic transition established by powder diffraction⁷.

The order parameter of the tetragonal to orthorhombic transition is proportional to the spontaneous deformation ϵ and can be fitted by a power law (upper panel in Fig. 5),

$$\epsilon = \frac{a-b}{a+b} = \tan\left(\frac{\gamma - 90^\circ}{2}\right) = A \left(1 - \frac{T}{T_s}\right)^\beta$$

with the critical exponent $\beta = 0.072(1)$ and a transition temperature of $T_s = 111(1)$ K.

The critical exponent is very small but comparable to the order parameters found for SrFe_2As_2 and EuFe_2As_2

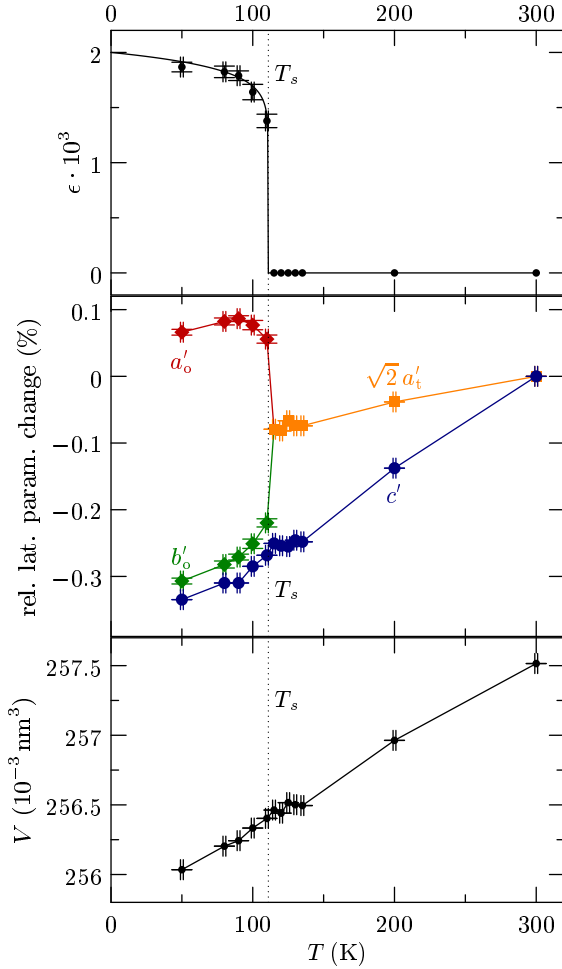


FIG. 5. (Color online) Temperature dependence of selected structural parameters of GdFeAsO single crystal. Error bars represent $\pm\sigma$. *Upper panel:* Spontaneous deformation fitted by a power law. *Middle panel:* Deviation of the lattice parameters relative to 300 K. ($a'_t = a_t/a_t(300\text{ K}) - 1$, $a'_o = a_o/[\sqrt{2}a_t(300\text{ K})] - 1$, $b'_o = b_o/[\sqrt{2}a_t(300\text{ K})] - 1$, and $c' = c/c(300\text{ K}) - 1$). *Lower Panel:* Cell volume of the orthorhombic phase and doubled volume of the tetragonal phase for comparison. Lines are guides for the eye in the middle and lower panel.

(0.098(1) and 0.112(1), respectively⁶), where structural and magnetic transition occur at the same temperature. Tegel *et al.* explained the small critical exponent by an ordering following the two-dimensional Ising model of the iron subsystem, which should yield a critical exponent of $1/8$. In the case of GdFeAsO the structural transition occurs at temperatures above the magnetic transition, which could be the reason for the even lower critical exponent determined, indicating that the structural transition of GdFeAsO is close to first order (concerning multiferroic transformation and the connection to first order phase transition see also Refs. 27 and 28).

The structural transition temperature $T_s = 111(1)\text{ K}$ obtained from the fit is lower than determined by Luo

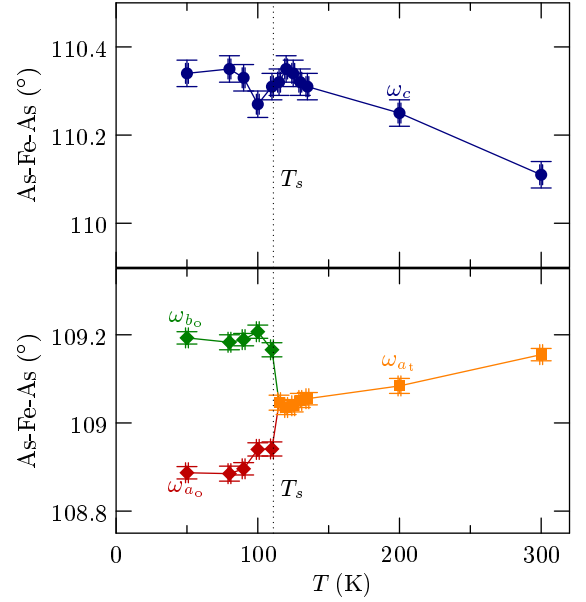


FIG. 6. (Color online) Temperature dependence of the As-Fe-As angles ω with its bisector parallel to the direction in subscript. Note the relation $\cos \omega_{a_t} = -\frac{1}{2}(1 + \cos \omega_c)$. Lines are guides for the eye, error bars represent $\pm\sigma$.

*et al.*⁹ with powder X-ray diffraction and resistivity measurements. This deviation might be caused by a systematic temperature error from the open flow helium cryostat used for this single-crystal X-ray diffraction study.

The lattice parameters and the volume of the tetragonal phase (middle and lower panel of Fig. 5) decrease in the course of cooling. However, there are hints that there is an anomaly just above the structural transition (e.g. different slope for c below 140 K), as it was also observed for the thermal expansion of GdFeAsO by Klingeler *et al.*¹¹ and assigned to a competition of differently ordered phases.

Interestingly, the height of the gadolinium atom above the oxygen layer (h_{Gd} in Fig. 1) remains almost constant over the whole temperature range, while the arsenic atom height over the iron layer (h_{As}) diminishes with decreasing lattice parameter c . The angle ω_c of the coordination polyhedron around Fe (Fig. 6) with its bisector parallel to the c -direction first increases upon cooling and then becomes almost constant already above the structural transition and does not change much upon further cooling. This indicates structural fluctuations by softening of the lattice or vibrational modes above the structural distortion which is also mirrored in other properties (e.g. thermal expansion¹¹ and X-ray reflection broadening²⁹). The angles with the angle bisector parallel a_o and b_o do not exhibit this anomaly and merely differentiate corresponding to the tetragonal to orthorhombic transition.

Although, the overall structural changes upon cooling are subtle, they indicate a response of the structure already at temperatures above the onset of the metric distortion. It is clear that higher resolution of the structural

investigations is needed to further study the interplay of structure and physical properties of both the “parent” and superconducting phases.

IV. CONCLUSION

A geometrical model was developed for single-crystal synchrotron X-ray diffraction measurements to quantify the metric distortion and twin formation of GdFeAsO induced by the tetragonal to orthorhombic structural transition.

Subtle changes in the structure are detectable. Fitting the spontaneous deformation by a power law lead to a small critical exponent of 0.072(1), which is lower than expected for a two-dimensional Ising model, pointing towards a transition close to first order. This may be caused by the separation of the magnetic and the structural transition in temperature. The lattice parameters decrease with decreasing temperature, and the a and b axes differentiate at temperatures below the structural transition. The deformation is abrupt and preceded by a stagnation of the decrease of the cell parameters. This

indicates long-range fluctuations of the lattice or softening of a vibrational mode at temperatures above the structural transition, which were also observed by other methods (e.g. Ref. 30). If this feature is linked to the superconductivity is not yet clear.

Although the presented structural information from single-crystal X-ray diffraction show the subtle structural changes around the tetragonal to orthorhombic phase transition, data with higher resolution is needed to unravel more details of the interplay of the structure and properties of the “parent” compounds of iron-based superconductivity.

V. ACKNOWLEDGEMENT

Parts of this research were carried out at the light source DORIS III at DESY, a member of the Helmholtz Association. We would like to thank Martin Tolkiehn and Mathias Herrmann for their assistance at beamline D3. The authors also like to thank Jutta Krug, Karoline Stolze, Eike Ahrens for their help with sample preparation and measurements.

-
- * thomas.doert@chemie.tu-dresden.de
- ¹ Y. Kamihara, H. Hiramatsu, M. Hirano, R. Kawamura, H. Yanagi, T. Kamiya, and H. Hosono, *J. Am. Chem. Soc.* **128**, 10012 (2006).
 - ² Y. Kamihara, T. Watanabe, M. Hirano, and H. Hosono, *J. Am. Chem. Soc.* **130**, 3296 (2008).
 - ³ J. Paglione and R. L. Greene, *Nat. Phys.* **6**, 645 (2010).
 - ⁴ T. Tohyama, *Jpn. J. Appl. Phys.* **51**, 010004 (2012).
 - ⁵ M. Rotter, M. Tegel, D. Johrendt, I. Schellenberg, W. Hermes, and R. Pöttgen, *Phys. Rev. B* **78**, 020503 (2008).
 - ⁶ M. Tegel, M. Rotter, V. Weiß, F. M. Schapacher, R. Pöttgen, and D. Johrendt, *J. Phys.: Condens. Matt.* **20**, 452201 (2008).
 - ⁷ C. de la Cruz, Q. Huang, J. W. Lynn, J. Li, W. R. II, J. L. Zarestky, H. A. Mook, G. F. Chen, J. L. Luo, N. L. Wang, and P. Dai, *Nature* **453**, 899 (2008).
 - ⁸ H.-H. Klauss, H. Luetkens, R. Klingeler, C. Hess, F. J. Litterst, M. Kraken, M. M. Korshunov, I. Eremin, S.-L. Drechsler, R. Khasanov, A. Amato, J. Hamann-Borrero, N. Leps, A. Kondrat, G. Behr, J. Werner, and B. Büchner, *Phys. Rev. Lett.* **101**, 077005 (2008).
 - ⁹ Y. Luo, Q. Tao, Y. Li, X. Lin, L. Li, G. Cao, Z.-A. Xu, Y. Xue, H. Kaneko, A. V. Savinkov, H. Suzuki, C. Fang, and J. Hu, *Phys. Rev. B* **80**, 224511 (2009).
 - ¹⁰ A. Jesche, C. Krellner, M. de Souza, M. Lang, and C. Geibel, *Phys. Rev. B* **81**, 134525 (2010).
 - ¹¹ R. Klingeler, L. Wang, U. Köhler, G. Behr, C. Hess, and B. Büchner, *J. Phys.: Conf. Ser.* **200**, 012088 (2010).
 - ¹² D. Johrendt, H. Hosono, R. Hoffmann, and R. Pöttgen, *Z. Kristallogr.* **226**, 435 (2011).
 - ¹³ M. A. Tanatar, A. Kreyssig, S. Nandi, N. Ni, S. L. Bud'ko, P. C. Canfield, A. I. Goldman, and R. Prozorov, *Phys. Rev. B* **79**, 180508 (2009).
 - ¹⁴ E. C. Blomberg, A. Kreyssig, M. A. Tanatar, R. M. Fernandes, M. G. Kim, A. Thaler, J. Schmalian, S. L. Bud'ko, P. C. Canfield, A. I. Goldman, and R. Prozorov, *Phys. Rev. B* **85**, 144509 (2012).
 - ¹⁵ C. Wang, L. Li, S. Chi, Z. Zhu, Z. Ren, Y. Li, Y. Wang, X. Lin, Y. Luo, S. Jiang, X. Xu, G. Cao, and Z. Xu, *Europhys. Lett.* **83**, 67006 (2008).
 - ¹⁶ C. Lee, A. Iyo, H. Eisaki, H. Kito, M. T. Fernandez-Diaz, T. Ito, K. Kihou, H. Matsuhata, M. Braden, and K. Yamada, *J. Phys. Soc. Japan* **77**, 083704 (2008).
 - ¹⁷ F. Nitsche, A. Jesche, E. Hieckmann, T. Doert, and M. Ruck, *Phys. Rev. B* **82**, 134514 (2010).
 - ¹⁸ “APEX2 (Version 2009.9),” (2009), Bruker AXS Inc.
 - ¹⁹ “SAINT+ (Version 7.68A),” (2009), Bruker AXS Inc.
 - ²⁰ G. M. Sheldrick, “SADABS (Version 2008/1),” (2008), Bruker AXS Inc.
 - ²¹ G. M. Sheldrick, *Acta Crystallogr. Sect. A* **64**, 112 (2007).
 - ²² Fachinformationszentrum Karlsruhe, D-76344 Eggenstein-Leopoldshafen, Germany, quote the depository numbers (CSD-No.) 425005 (300 K), 425006 (200 K), 425007 (135 K), 425008 (130 K), 425009 (125 K), 425010 (120 K), 425011 (115 K), 425012 (110 K), 425013 (1100 K), 425014 (90 K), 425015 (80 K), and 425016 (50 K).
 - ²³ “MATLAB (Version 7.12.0.635 R2011a),” (2011), The MathWorks Inc.
 - ²⁴ S. Kotz and S. Nadarajah, *Multivariate T-Distributions and Their Applications* (Cambridge University Press, 2004).
 - ²⁵ G. J. McIntyre and D. Visser, *J. Phys. Colloques* **47**, 75 (1986).
 - ²⁶ G. J. McIntyre, A. Renault, and G. Collin, *Phys. Rev. B* **37**, 5148 (1988).
 - ²⁷ A. E. Jacobs, *Phys. Rev. B* **61**, 6587 (2000).

- ²⁸ E. K. H. Salje and M. A. Carpenter, J. Phys.: Condens. Matter **23**, 462202 (2011).
- ²⁹ M. A. McGuire, A. D. Christianson, A. S. Sefat, B. C. Sales, M. D. Lumsden, R. Jin, E. A. Payzant, D. Mandrus, Y. Luan, V. Keppens, V. Varadarajan, J. W. Brill, R. P. Hermann, M. T. Sougrati, F. Grandjean, and G. J. Long, Phys. Rev. B **78**, 094517 (2008).
- ³⁰ S. E. Hahn, G. S. Tucker, J.-Q. Yan, A. H. Said, B. M. Leu, R. W. McCallum, E. E. Alp, T. A. Lograsso, R. J. McQueeney, and B. N. Harmon, “Magnetism dependent phonon anomaly in LaFeAsO observed via inelastic x-ray scattering,” (2012), arXiv:cond-mat/1206.1096.